Determination of dipping contacts using electrical resistivity tomography

René PUTIŠKA[1], Ivan DOSTÁL[1], David KUŠNIRÁK[1]

[1] Department of Applied and Environmental Geophysics, Faculty of Natural Sciences
Comenius University, Mlynská dolina, pav. G, 842 48 Bratislava, Slovak Republic
e-mail: putiska@fns.uniba.sk; dostal@fns.uniba.sk; kusnirak@fns.uniba.sk

Abstract: Generally, all electrode arrays are able to delineate the contact of two lithostratigraphic units especially with very high resistivity contrast. However, the image resolution for the location of vertical and dipping structures is different. The responses of dipole-dipole (DD), Wenner alpha (WA), Schlumberger (SCH) and combined pole-dipole (PD) arrays have been computed using the finite difference method. Comparison of the responses indicates that: (1) The dipole-dipole array usually gives the best resolution and is the most detailed method especially for the detection of vertical structures. This array has shown the best resolution to recognize the geometrical characterisation of the fault. (2) The pole-dipole has shown the second best result in our test. The PD is an effective method for detection of vertical structures with a high depth range, but the deepest parts are deformed. (3) Wenner alpha shows a low resolution, inconvenient for detailed investigation of dip structures. (4) The Schlumberger array gives a good and sharp resolution to assess the contact between two lithological units but gives poor result for imaging geometry of dipping contact.

Key words: electrical resistivity tomography, **L_2 norm** inversion method, **L_1 norm** inversion method, vertical and dipping contact

1. Introduction

The resistivity tomography is a common method to indicate vertical structures *(Caputo et al., 2003; Wise et al., 2003; Rizzo et al., 2004; Nguyen et al., 2005* and *Fazzito et al., 2009)* and others, but what is the possibility of the method to determine angle of the dipping contact? For investigation of this problem we defined 2D subsurface model with three different angles $60°$, $90°$ and $120°$ which were investigated through a numerical modelling. A variety of electrode arrays are available for exploration using the resistivity tomography. Comparison of the responses of dipole-dipole (DD), Wenner

alpha (WA), Schlumberger (SCH), combined pole-dipole (PD) arrays have been computed using the finite difference method.

The choice of the "best" array for a field resistivity survey depends on the type of structure to be mapped, the sensitivity of the resistivity meter and the background noise level. Each type of combination has advantages and limitations in terms of lateral resolution and vertical penetration for instance.

2. The synthetic test

The main goal of this study is the ability of electrical tomography to make a visual estimation for direction and slope of vertical contact. In order to assess the trend of dip, the following has been carried out to compare the effect of the inversion method.

The synthetic data are computed using the forward modelling program RES2DMOD *(Loke and Barker, 1996)*, with no Gaussian noise added to the data sets. The synthetic models used in this work represent the three geometrical settings of the contact of two geological environments (a vertical $90°$ and a dipping $60°$ and $120°$) and they represent a simplified geological and structural sketch along the profile (Fig. 3a, 6a, 9a). These models have been saved as the data of the apparent resistivity without topographic information. Synthetic data sets were generated for dipole-dipole (DD), Wenner alpha (WA), Schlumberger (SCH), combined pole-dipole (PD) arrays with an electrode spacing of 5.5 m.

Firstly, three models with a difference in the thickness and number of the model layers were compared (Fig. 1b, c, d). The RES2DINV *(Loke and Barker, 1996)* program generated size and positions of the model blocks *(Loke, 1997)*. The model (Fig. 1a) has subdivided the subsurface into rectangular blocks with varying resistivity *(Loke and Barker, 1995)*, the overview of the main parameters of models is compiled in Table 1.

For inversion process the software RES2DINV among others use inversion methods as **L_2 norm**, **L_1 norm** with standard horizontal and vertical roughness filter and **L_1 norm** with diagonal roughness filter.

The **L_2 norm** inversion method gives optimal results where the subsurface geology exhibits a smooth variation, such as the diffusion boundary of

Table 1. Model parameters of the three models used in the synthetic test

	Model A	Model B	Model C
Number of data points	1035	1035	1035
Ratio of thickness of the first layer	1.5	0.8	0.3
Factor to increase layer thickness with depth	1.1	1.1	1.1
Number of blocks	206	310	1506
Number of models layers	6	10	23

a chemical plume. However, in cases where the subsurface consists of bodies that are internally homogeneous with sharp boundaries (such as an igneous dyke), this method tends to smear out the boundaries. The **L_1 norm** or blocky optimisation method tends to produce models that are piecewise constant *(Ellis and Oldenburg, 1994)*. The data sets have been inverted using the **L_2 norm** inversion method (Fig. 1h, i, j), **L_1 norm** with standard horizontal and vertical roughness filter (Fig. 1e, f, g), and **L_1 norm** with diagonal roughness filter (Fig. 1k, l, m).

The results show that for the **L_1 norm** inversion method it is better to use a model where the number of model cells exceeds the number of data points *(Loke et al., 2003)*, what eliminates the effect of the block (Fig. 1g, m). The robust inversion with wide model blocks gave images that were too 'blocky' (Fig. 1e, f, k, l). In case of the **L_2 norm** inversion method very wide cells reduce the effect of smoothness (Fig. 1h, i, j).

In the next work phase a model C has been used (Fig. 1d, Table 1). During further analysis the effect of three different factors able to influence the result was tested:

1. resistivity contact of two different lithological units with varying angle of the dip (60, 90 and 120 degrees),
2. type of electrode array to investigate the imaging capabilities of these electrode configurations,
3. effect of the inversion method (**L_2 norm** inversion method, **L_1 norm** with standard horizontal and vertical roughness filter and **L_1 norm** with diagonal roughness filter) to define the dip of tectonic fault (60, 90 and 120 degrees).
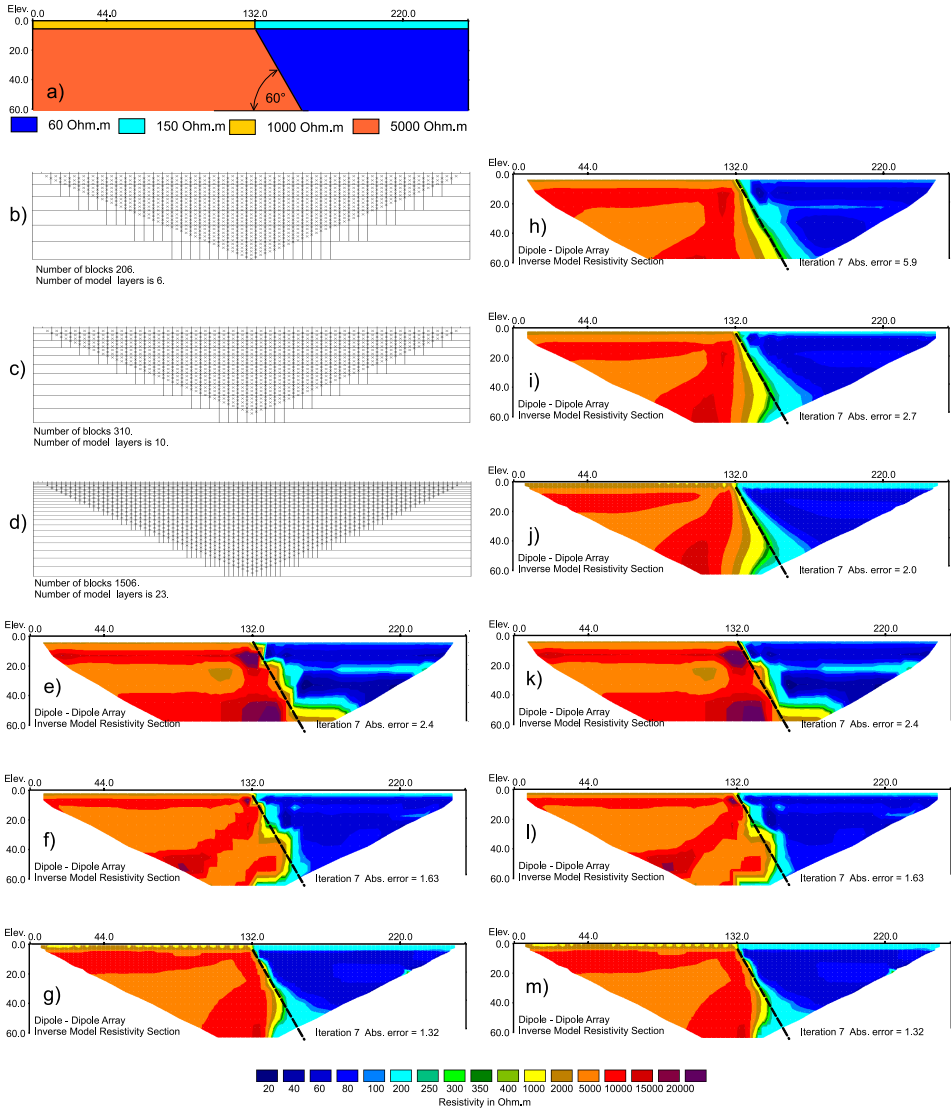
Fig. 1. The effect of models with different methods to subdivide the subsurface into rectangular prisms on the inversion result: a) geometry of synthetic model; b, c, d) arrangement of model blocks and apparent resistivity data points; e, f, g) inverse model using the L_1 norm with standard horizontal and vertical roughness filter; h, i, j) inverse model using the L_2 norm inversion method; k, l, m) inverse model using the L_1 norm with diagonal roughness filter.

164

The results of the work are shown in Fig. 3–11. The pictures show a set of inversion models with different arrays configuration and different inversion parameters. The inversion models are calculated from synthetic data with vertical contact (90 degrees – Fig. 3, 4, 5) and dipping contact (60 degrees – Fig. 6, 7, 8 or 120 degrees – Fig. 9, 10, 11).

3. Electrical arrays

Generally, all tested electrode arrays (Fig. 2) are able to delineate the contact of two lithostratigraphic units especially with very high resistivity contrast. However, the image resolution for the location of vertical and dipping structures is different.

Based on the numerical simulations, it is possible to summarize the main advantages and disadvantages of these arrays when assessing the dip of the fault. These electrode configurations were also investigated using robust (**L_1 norm**) inversion and smoothness-constrained least-squares (**L_2 norm**) inversion *(Farquharson, 2008)* for the three synthetic models.

Dipole-Dipole (DD) is the most detailed method especially for the detection of vertical structures. This array has shown the best resolution to recognize the geometrical characterisation of the fault. The depth range of this array is about 1/5 of the maximum C2P2 distance used. The effective depth range is strongly limited by a rapid decrease of the measured potential at larger dipole distance. Artificial electric noise causes additional significant limitation on the use of this method. The highest resolution allows

Wenner Alpha   **Dipole - Dipole**

C1 a P1 a P2 a C2   C2 a C1 na P1 a P2

Schlumberger   **Pole - Dipole**

C1 na P1 a P2 na C2   C1 na P1 a P2

C1, C2 - current electrodes   a - dipole length
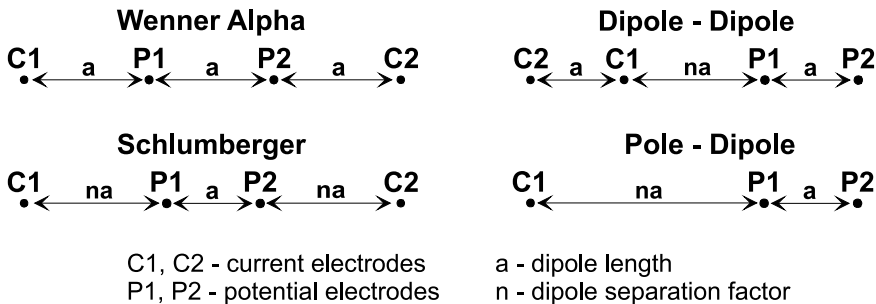P1, P2 - potential electrodes   n - dipole separation factor

Fig. 2. The arrays used in resistivity test and their geometric factors.

the maximum possible differentiation of deeper situated structures, but the deeper structures may be deformed (Fig. 3b–11b).

The combined Pole-Dipole (PD) array has shown the second best result in our test. The PD is an effective method for detection of vertical structures with a high depth range, but the deepest parts are deformed. Section coverage is about 1/3 of the used length of the electrode array. The accuracy of positions in section decreases (side shift) with depth Fig. 3c–11c. This array requires the installation of an external current electrode C2 (C1 in case of a reverse way) – called the infinite electrode. The place of the infinite electrode must be at least at the distance of fivefold of the maximum length of the used electrode array. Its optimum position should be in the perpendicular direction from the electrode array. The long distance of the infinite current electrode requires a maximum power of the transmitter and a careful installation of such an electrode (or even electrode nest) to reach its lowest possible ground resistance.

The Wenner alpha (WA) array has a low depth range (about 1/6 of the maximum used C1C2 distance) and a low side covering. The results of this array show a low resolution, inconvenient for detailed investigation of dip structures because all models show more or less vertical contact without the geometry of dip Fig. 3d–11d.

Schlumberger (SCH) is suited especially for depicting horizontal and sub-horizontal (declined) layers. Detection of larger inhomogeneities of various shape and direction like wider crackles, tectonic zones and contacts of layers with difference of resistivities is also effective. This array gives a good and sharp resolution to assess the contact between two lithological units but a poor result of imaging geometry of dipping contact (Fig. 3e–11e). Section covering of this array is about 1/5 of the maximum used C1C2 distance and the resolution is medium sufficient, rather for detailed investigation of shallow structures.

4. Test results

The **L_2 norm** smoothness-constrained optimization method produces a model with a smooth variation of resistivity values. After the comparison of DD, PD, WA and WS results, it is possible to say that the contact between the lithological units is not sharp enough to assess the exact dip
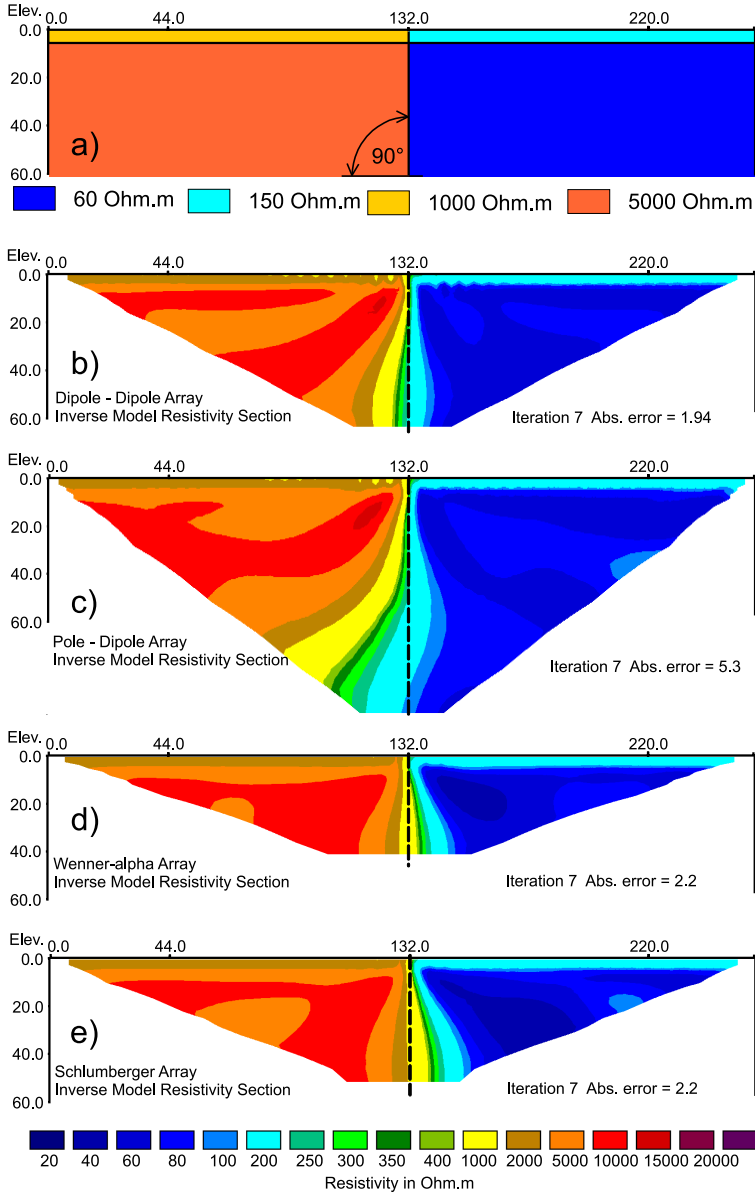
Fig. 3. Inverse model resistivity sections from synthetic data set (using the **L₂ norm** inversion method): a) geometry of the synthetic model, b) dipole-dipole array, c) pole-dipole array, d) Wenner-alpha array, e) Schlumberger array.
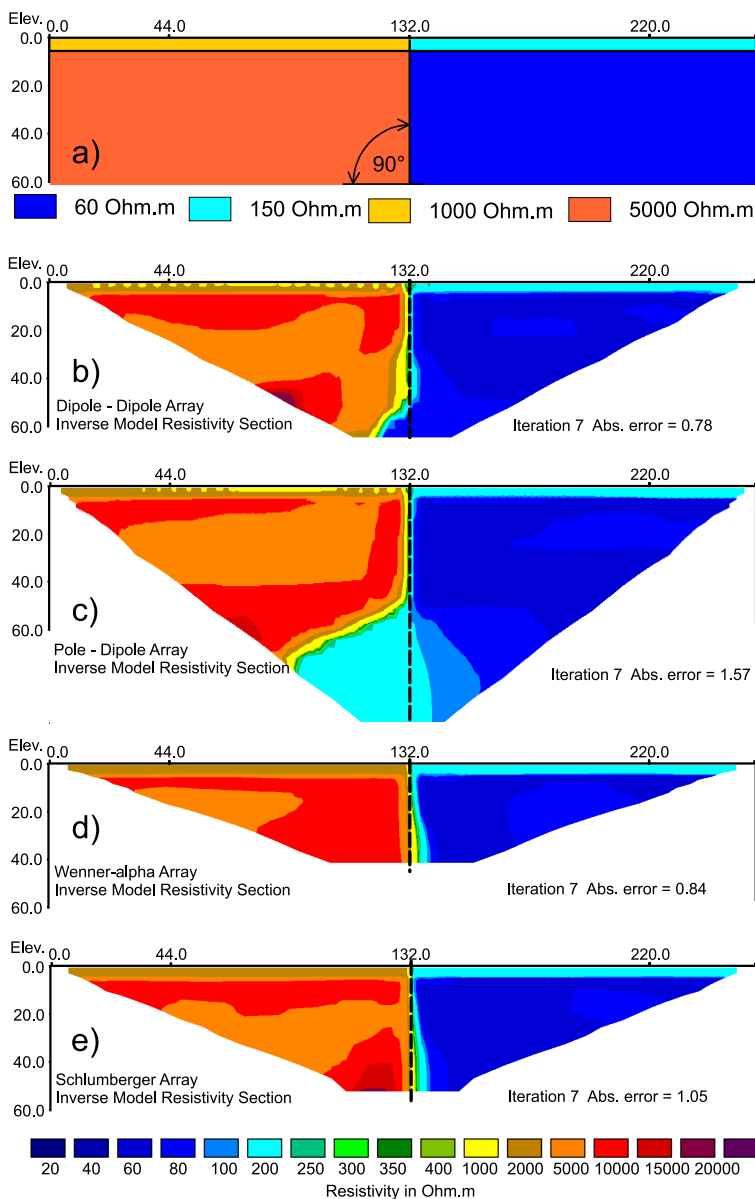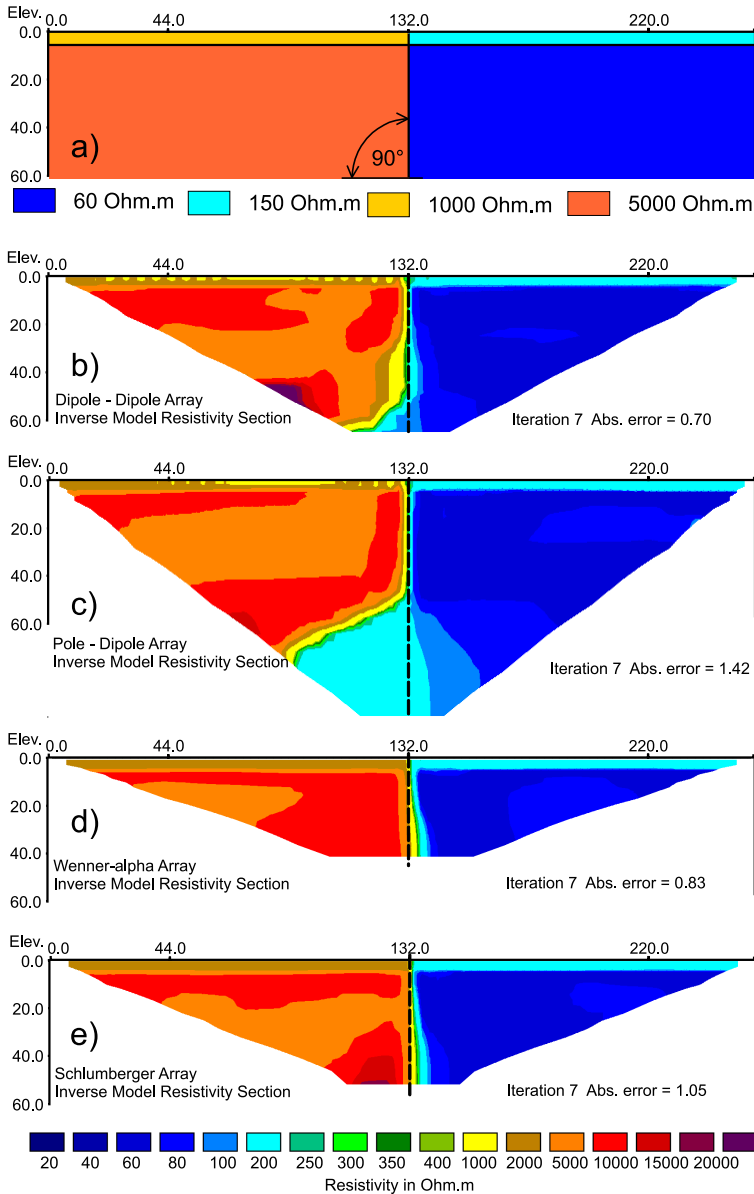
Fig. 4. Inverse model resistivity sections from synthetic data set (using the **L₁ norm** with standard horizontal and vertical roughness filter): a) geometry of the synthetic model, b) dipole-dipole array, c) pole-dipole array, d) Wenner-alpha array, e) Schlumberger array.
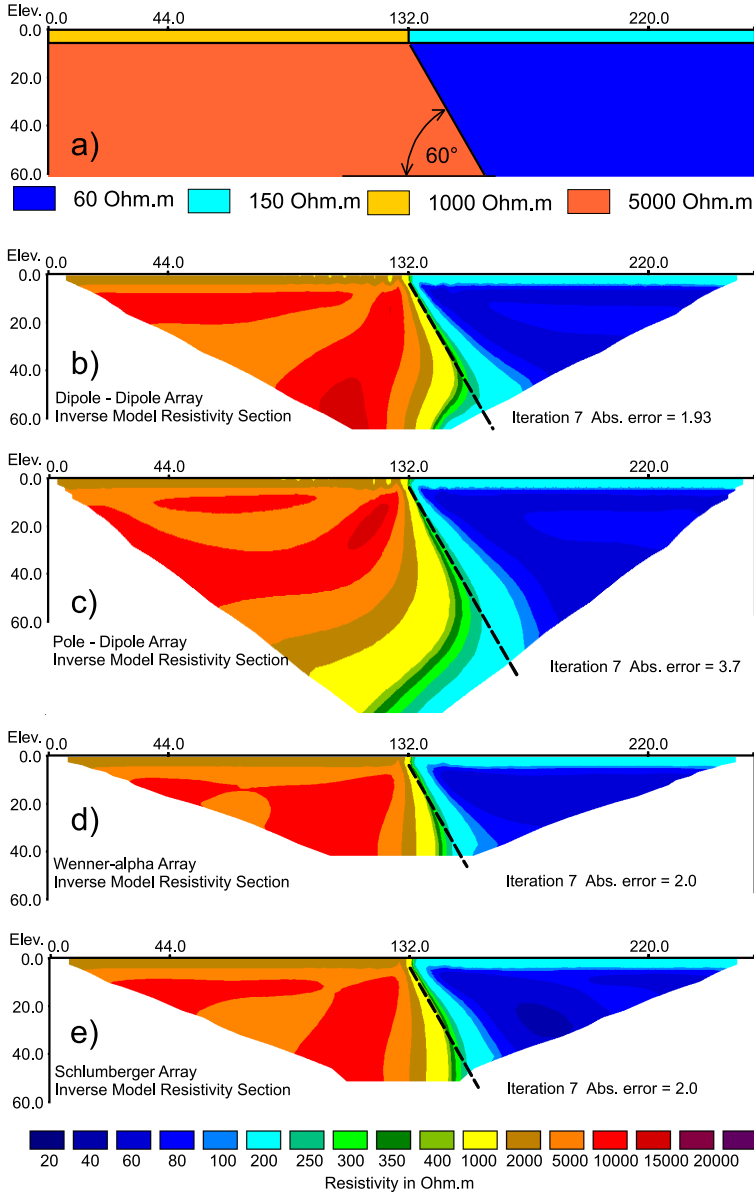
Fig. 5. Inverse model resistivity sections from synthetic data set (using the **L₁ norm** with diagonal roughness filter): a) geometry of the synthetic model, b) dipole-dipole array, c) pole-dipole array, d) Wenner-alpha array, e) Schlumberger array.

169

Fig. 6. Inverse model resistivity sections from synthetic data set (using the **L₂ norm** inversion method): a) geometry of the synthetic model, b) dipole-dipole array, c) pole-dipole array, d) Wenner-alpha array, e) Schlumberger array.
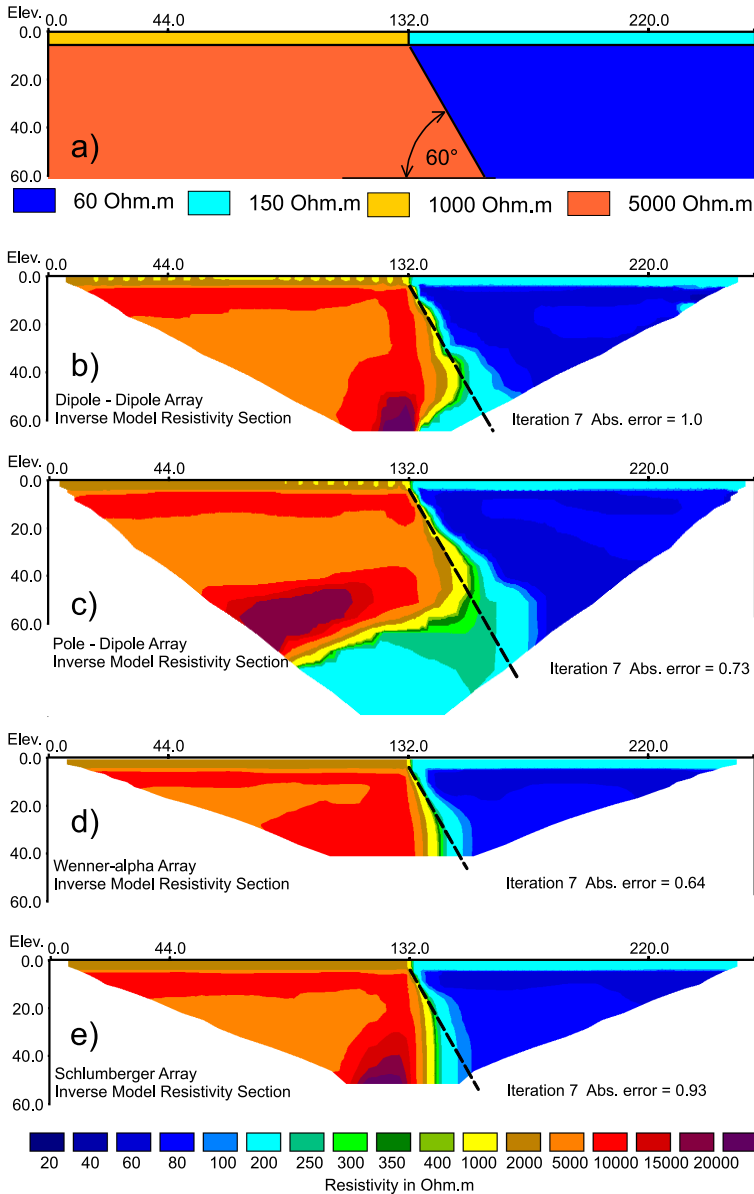
Fig. 7. Inverse model resistivity sections from synthetic data set (using the **L₁ norm** with standard horizontal and vertical roughness filter): a) geometry of the synthetic model, b) dipole-dipole array, c) pole-dipole array, d) Wenner-alpha array, e) Schlumberger array.
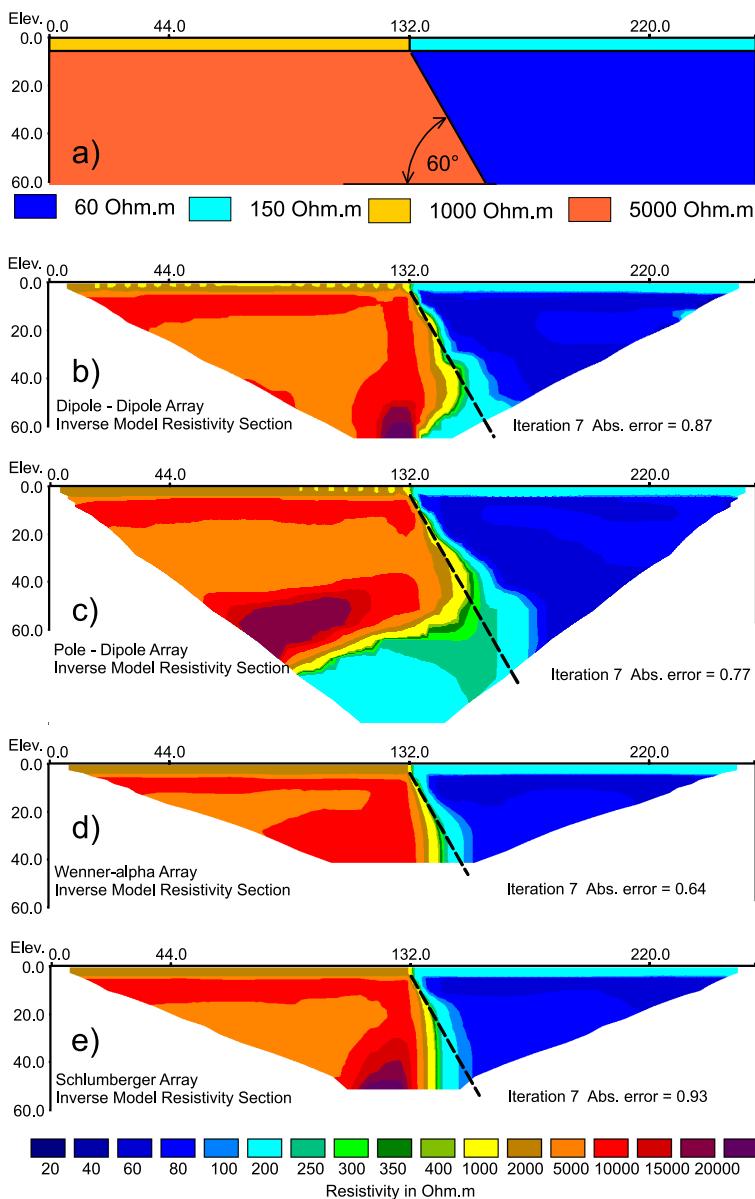
171

Fig. 8. Inverse model resistivity sections from synthetic data set (using the **L₁ norm** with diagonal roughness filter): a) geometry of the synthetic model, b) dipole-dipole array, c) pole-dipole array, d) Wenner-alpha array, e) Schlumberger array.
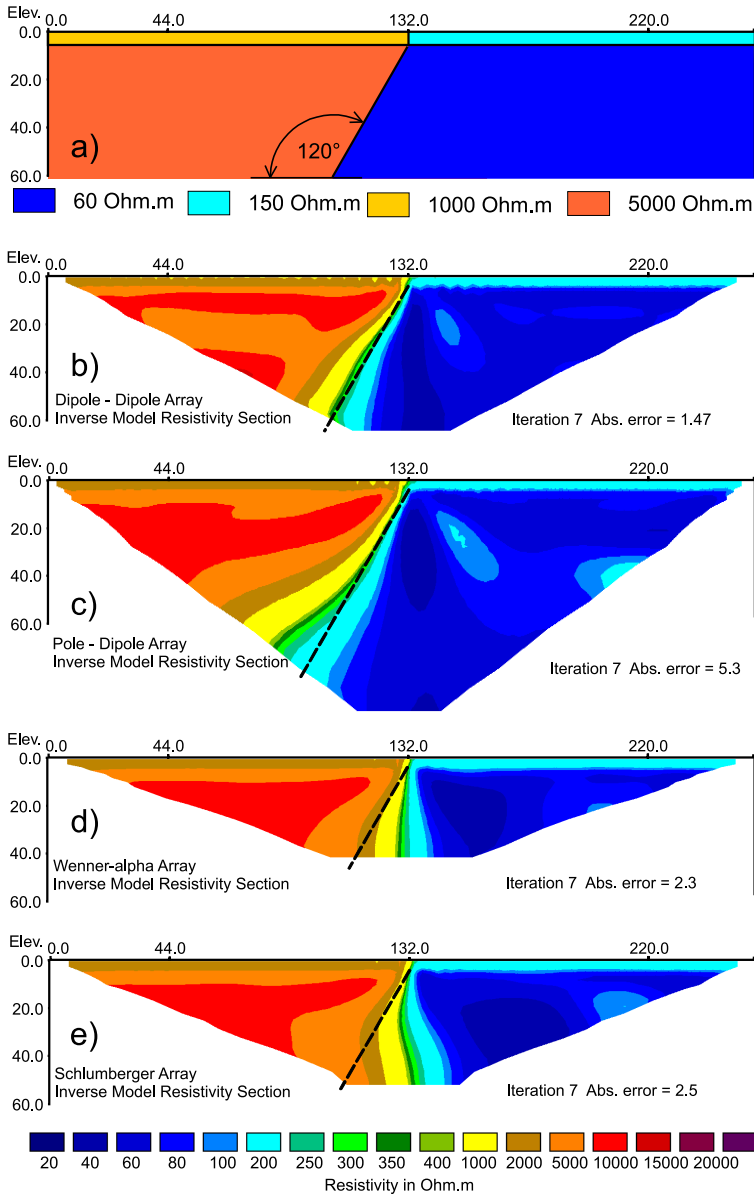
Fig. 9. Inverse model resistivity sections from synthetic data set (using the **L₂ norm** inversion method): a) geometry of synthetic the model, b) dipole-dipole array, c) pole-dipole array, d) Wenner-alpha array, e) Schlumberger array.
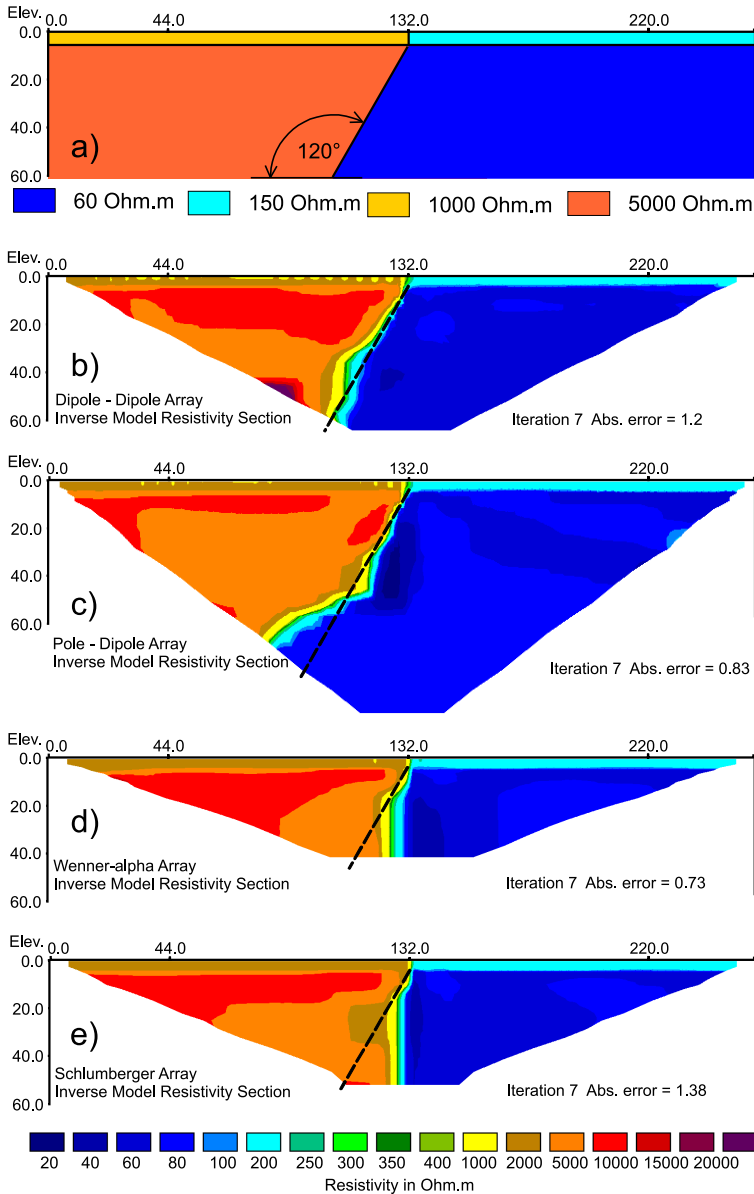
173

Fig. 10. Inverse model resistivity sections from synthetic data set (using the **L₁ norm** with standard horizontal and vertical roughness filter): a) geometry of the synthetic model, b) dipole-dipole array, c) pole-dipole array, d) Wenner-alpha array, e) Schlumberger array.

Fig. 11. Inverse model resistivity sections from synthetic data set (using the **L₁ norm** with diagonal roughness filter): a) geometry of the synthetic model, b) dipole-dipole array, c) pole-dipole array, d) Wenner-alpha array, e) Schlumberger array.
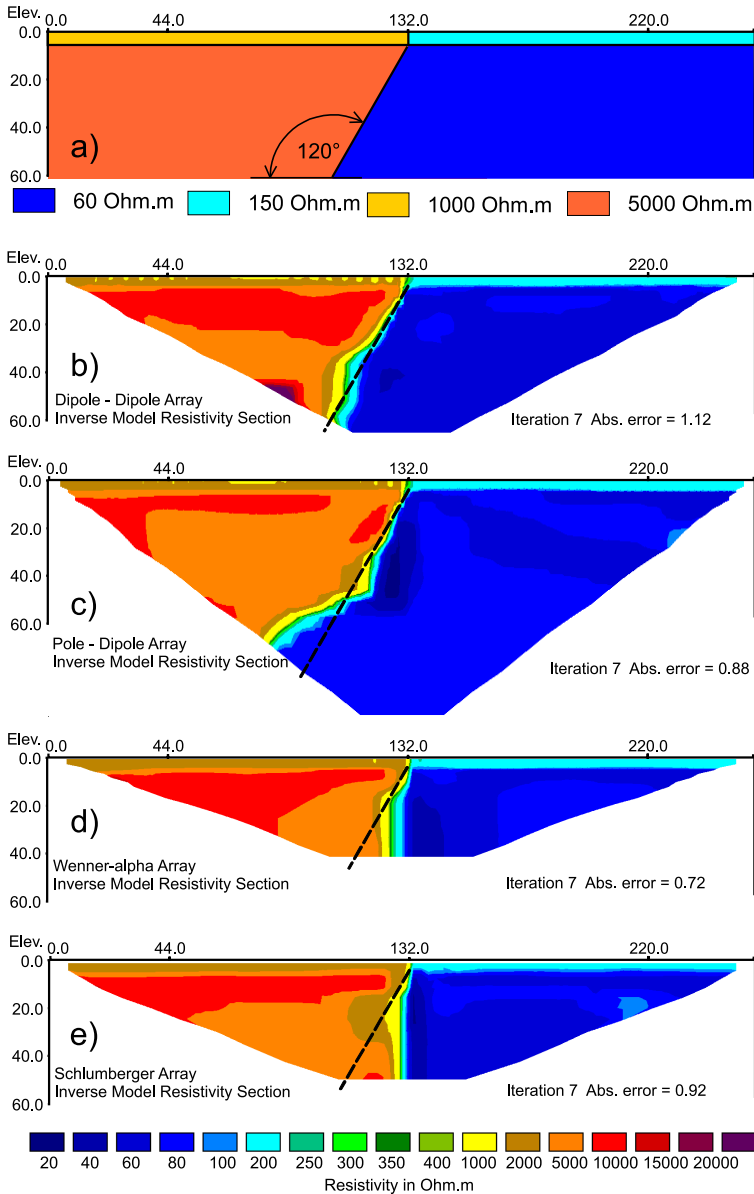
175

of the fault, even if the number of model cells exceeds the number of data points. The L_2 **norm** smooth inversion method is not optimal for such data sets (Fig. 3, 6, 9). The L_2 **norm** inversion method gives the optimal results where the subsurface geology shows a smooth variation, such as the diffusion boundary of a chemical plume. However, in cases where the subsurface consists of bodies that are internally homogeneous with sharp boundaries (such as an igneous dyke), this method tends to smear out the boundaries *(Loke et al., 2010)*.

In this case the L_1 **norm** with standard horizontal and vertical roughness filter (Fig. 4, 7, 10) gave different results for each of the arrays used. For DD (Fig. 4b, 7b, 10b) and PD (Fig. 4c, 7c, 10c) the model contains sharp dipping and vertical interface with some deformations on the bottom. The WA (Fig. 4d, 7d, 10d) and SCH (Fig. 4e, 7e, 10e) result show a sharp vertical interface but these two arrays are not able to recognize the geometry of dip.

In case of the L_1 **norm** with diagonal roughness filter the finite-element method with triangular elements was used for the forward modelling calculation (Fig. 5, 8, 11). On the Fig. 1 are shown models with different number of blocks but with the same number of data points (Table 1).

The RMS error resulting from the inverse model calculation for all three mentioned inverse methods has been used as a quantitative tool to compare the suitability of the inversion method (Fig. 12). An RMS error parameter has been normalized to 1000 points of the input model.

The model A arrangement shows 206 numbers of blocks. This model has been inverted using the L_2 **norm** inversion method (Fig. 1h), the L_1 **norm** with standard horizontal and vertical roughness filter (Fig. 1e) and the L_1 **norm** with diagonal roughness filter (Fig. 1k). Figure 1k shows the resulting model, when the diagonal finite elements were given more importance than the horizontal and vertical differences (Fig. 1e).

The third model arrangement shows 1506 numbers of blocks. In this case the number of model cells exceeds the number of data points. The differences between the L_1 **norm** with standard horizontal and vertical roughness filter (Fig. 1g) and the L_1 **norm** with diagonal roughness filter (Fig. 1m) are not significant – both methods give very similar results (Fig. 4, 5, 7, 8, 10, 11).

From the results of the test we can state several outputs:

1. each of the involved electrical arrays is able to identify resistivity contact between two lithological layers, but with increasing depth the reso-
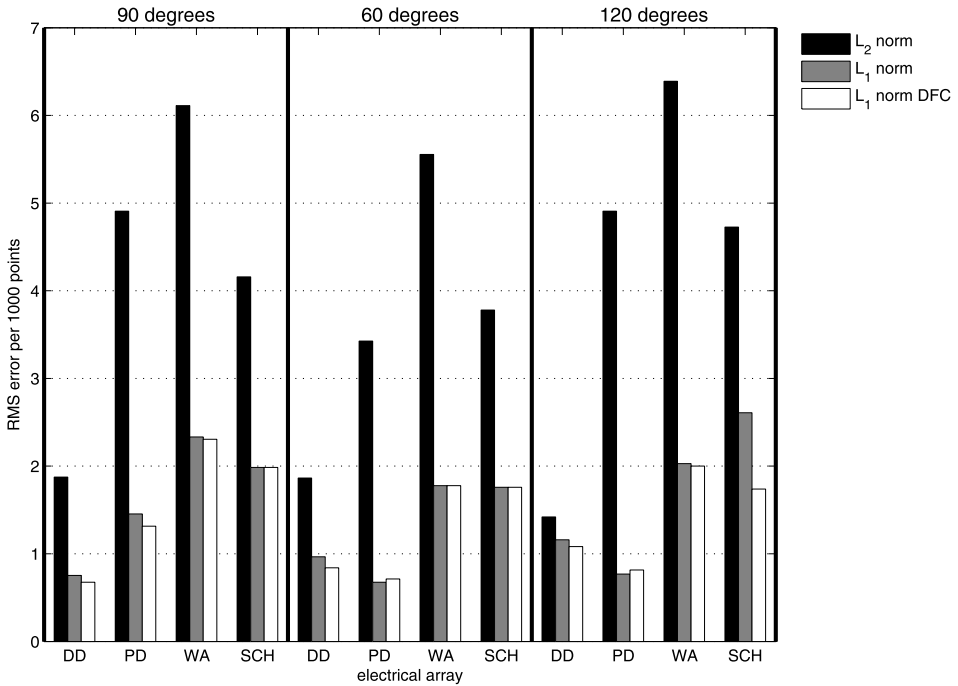
Fig. 12. RMS error comparison resulted from the inversion of the models. The error is normalised per 1000 points of the model for all electrical arrays involved in test – the Dipole-Dipole (DD), combined Pole-Dipole (PD), Wenner alpha (WA) and Wenner-Schlumberger (SCH). All three contact variants with 90 degrees, 60 degrees and 120 degrees angle of the dip were calculated using **L₂ norm** and **L₁ norm** with standard settings and also with diagonal filter components (**L₁ norm**, DFC).

lution of the inverse model does not allow to recognize sharp boundary between the layers. The effect is caused by the lower density of the measured points in deeper parts of the image.

2. reliable quantitative estimation of the angle between the lithological layers combined Pole-Dipole (PD) and Dipole-Dipole shows best results unlike WA and SCH do.

3. effect of the selected inversion method is significant to the final inversion model as the **L₁ norm** with diagonal filter components gives in most of the cases best results (Fig. 12).

Table 2. Summarized results from the synthetic test for each electrode array

Array / Description	Wenner-Schlumberger	Wenner alpha	Dipole-Dipole	combined Pole-Dipole
Purpose	Detection of larger inhomogenities of various shape and direction like wider crackes, tectonic zones, ore veins and contacts of layers with big difference of resistivities is also effective.	The most frequent variant called Wenner alpha is close to Schlumberger with similar range of applications.	The most detailed method especially for detection of vertical structures (including slimmer fissures, ore veins) and cavities.	The most effective method for detection of all vertical structures with high depth range.
Section covering	Medium depth range - of about 1/4 of the maximum used C1C2 distance. Medium side covering.	Low depth range – of about 1/6 of the maximum used C1C2 distance. Low side covering.	Medium depth range- of about 1/5 of the maximum used C1C2 distance. Medium covering.	High depth range – of about 1/3 of the used length of the electrode array. Higher side covering.
Resolution	Medium resolution – inconvenient for detailed investigation of deeper structures.	Low resolution – inconvenient for detailed investigation of deeper structures.	The highest resolution – allows the maximum possible distinguishing of deeper situated structures.	Higher resolution. The accuracy of positions in section is decreased (side shift) as the method is non symmetric.
Measuring conditions	High resistance against electric noise.	High resistance against electric noise.	The effective depth range is strongly limited by rapid decrease of measured potential at larger dipole distance.	Installation of external current electrod C2 (C1) – called infinite – is necessary.

178

5. Conclusions

A synthetic test allows us to compare the capabilities of the selected electrode array and inversion settings to identify a dipped contact of two geological layers and estimate the real angle between them. The data have been calculated by the **L_2 norm** inversion method, the **L_1 norm** with standard horizontal and vertical roughness filter and the **L_1 norm** with diagonal roughness filter. The 2D inversion result of the resistivity profile correlated with synthetic models. From these synthetic models it is possible to summarize the main advantages or disadvantages of these arrays for 2D resistivity imaging compiled in Table 2.

References

Caputo R., Piscitelli S., Oliveto A., Rizzo E., Lapenna V., 2003: The use of electrical resistivity tomographies in active tectonics: examples from Tyrnavos Basin, Greece. Journal of Geodynamics, **36**, 19–35.

Ellis R. G., Oldenburg D. W., 1994: Applied geophysical inversion. Geophysical Journal International, **116**, 5–11.

Farquharson C. G., 2008: Constructing piecewise-constant models in multidimensional minimum- structure inversions. Geophysics, **73**, K1–K9.

Fazzito S. Y., Rapalini A. E., Cortés J. M., Terrizzano C. M., 2009: Characterization of Quaternary faults by electric resistivity tomography in the Andean Precordillera of Western Argentina. Journal of South American Earth Sciences, **28**, 217–228.

Loke M. H, Barker R. D., 1995: Least-squares deconvolution of apparent resistivity pseudosection. Geophysics, **60**, 1682–1690.

Loke M. H., Barker R. D., 1996: Rapid least-squares inversion of apparent resistivity pseudosections by a quasi-Newton method. Geophysical Prospecting, **44**, 131–152.

Loke M. H., 1997: Rapid 2D resistivity inversion using the least-squares method, RES2 DINV Program manual, Penang, Malaysia.

Loke M. H., Acworth I., Dahlin T., 2003: A comparison of smooth and blocky inversion methods in 2D electrical imaging surveys. Exploration Geophysics, **34**, 182–187.

Loke M. H., Wilkinson P. B., Chambers J. E., 2010: Fast computation of optimized electrode arrays for 2D resistivity surveys. Computers and Geosciences, **36**, 11, 1414–1426.

Nguyen F., Garambois S., Jongmans D., Pirard E., Loke M. H., 2005: Image processing of 2D resistivity data for imaging faults. Journal of Applied Geophysics, **57**, 260–277.

Rizzo E., Colella A., Lapenna V., Piscitelli S., 2004: High-resolution images of the fault-controlled high agri valley basin (Southern Italy) with deep and shallow electrical resistivity tomographies. Physics and Chemistry of the Earth, **29**, 321–327.

Wise D. J., Cassidy J., Locke C. A., 2003: Geophysical imaging of the quaternary Wairoa North Fault, New Zealand: a case study. Journal of Applied Geophysics, **53**, 1–16.